nature photonics

LETTERS

PUBLISHED ONLINE: 7 DECEMBER 2008 | DOI: 10.1038/NPHOTON.2008.247

Monolithic germanium/silicon avalanche photodiodes with 340 GHz gain–bandwidth product

Yimin Kang[1]*, Han-Din Liu[1,5], Mike Morse[1], Mario J. Paniccia[1], Moshe Zadka[2], Stas Litski[2], Gadi Sarid[2], Alexandre Pauchard[3], Ying-Hao Kuo[4], Hui-Wen Chen[4], Wissem Sfar Zaoui[4], John E. Bowers[4], Andreas Beling[5], Dion C. McIntosh[5], Xiaoguang Zheng[5] and Joe C. Campbell[5]

Significant progress has been made recently in demonstrating that silicon photonics is a promising technology for low-cost optical detectors, modulators and light sources[1–12]. It has often been assumed, however, that their performance is inferior to InP-based devices. Although this is true in most cases, one of the exceptions is the area of avalanche photodetectors, where silicon's material properties allow for high gain with less excess noise than InP-based avalanche photodetectors and a theoretical sensitivity improvement of 3 dB or more. Here, we report a monolithically grown germanium/silicon avalanche photodetector with a gain–bandwidth product of 340 GHz, a k_{eff} of 0.09 and a sensitivity of −28 dB m at 10 Gb s^{-1}. This is the highest reported gain–bandwidth product for any avalanche photodetector operating at 1,300 nm and a sensitivity that is equivalent to mature, commercially available III–V compound avalanche photodetectors. This work paves the way for the future development of low-cost, CMOS-based germanium/silicon avalanche photodetectors operating at data rates of 40 Gb s^{-1} or higher.

Avalanche photodetectors (APDs) are widely used in fibre-optic communications where high sensitivities are needed. Traditional InP-based APD receivers typically offer a 10-dB improvement in sensitivity at 10 Gb s^{-1} when compared to standard p–i–n-based receivers. As the data rate increases above 10 Gb s^{-1}, however, the limited gain–bandwidth product of standard InP APDs (∼100 GHz) results in degraded receiver sensitivity. In order to overcome this limitation, an increasing amount of research is now focusing on alternative multiplication materials for APDs, and one of the most promising is silicon. The difficulty in realizing a silicon-based APD device at near-infrared wavelengths is that a compatible absorbing material is difficult to find. The leading candidate is germanium, and research on germanium/silicon p–i–n detectors has shown good responsivity at wavelengths up to 1,550 nm (ref. 7), although the 4% lattice mismatch can result in a high concentration of dislocations and dark current. However, careful processing and device design can minimize the impact of the dislocations. The work presented here extends the research on germanium/silicon p–i–n detectors to the development of a more sensitive APD structure.

The key material property that determines the gain–bandwidth product and the excess noise of an APD is the effective k ratio of the ionization coefficients of electrons and holes. A low k value is desirable for high-performance APDs[13,14]. Conventional III–V APDs use InP ($k \approx 0.4–0.5$) (refs 15,16) or InAlAs ($k \approx 0.1–0.2$) (refs 17,18) for the multiplication region. Recent work has shown that by taking advantage of the dead space effect with a 150-nm-thick InAlAs multiplication layer, a gain–bandwidth product of 320 GHz can be achieved[17], but at the expense of an impractically low quantum efficiency of 16%.

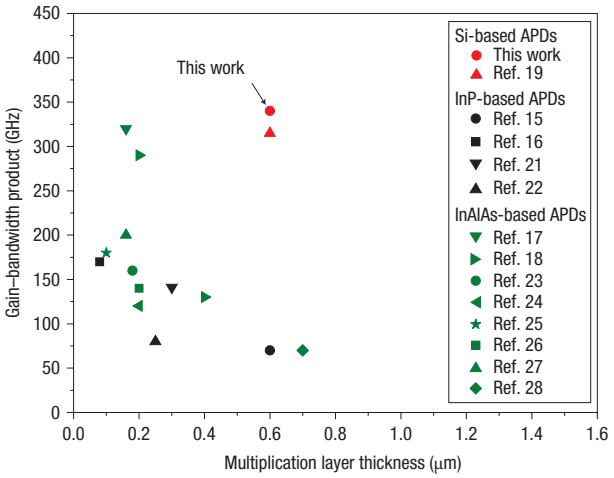

Figure 1 | Summary of published gain–bandwidth products with respect to the multiplication layer thickness for InP-, InAlAs- and silicon-based APDs. The black symbols are measured values for InP-based APDs[15,16,21,22], the green symbols for InAlAs-based APDs[17,18,23–28] and the red symbols for silicon-based APDs including InGaAs/Si APD[19] (red triangle) and the monolithic germanium/silicon device presented in this paper (red circle).

Silicon has been studied for several decades and is well known for its low k value ($k < 0.1$). Promising results obtained from InGaAs/Si APDs fabricated using wafer bonding technology indicate that it is possible to combine the low-noise properties of silicon with the high absorption properties of III–V materials at telecom wavelengths. These devices had a gain–bandwidth product of 315 GHz (ref. 19) and a k-value of 0.02 (ref. 20). Although these were promising results, the wafer bonding technology would have the extra expense of III–V epitaxial wafers and the challenge of inserting III–V materials into a silicon CMOS fabrication facility. A more ideal approach would be to develop an APD based on a monolithic, CMOS-compatible process.

[1]Intel Corporation, 2200 Mission College Boulevard, Santa Clara, California 95054, USA, [2]Numonyx, 2 Tzoran Boulevard, Qiryat-Gat 82109, Israel, [3]Chemin de Crey-Derrey 152, 1618 Châtel-St-Denis, Switzerland, [4]University of California Santa Barbara, ECE Department, Santa Barbara, California 93106, USA, [5]University of Virginia, ECE Department, Charlottesville, Virginia 22904, USA; *e-mail: yimin.kang@intel.com

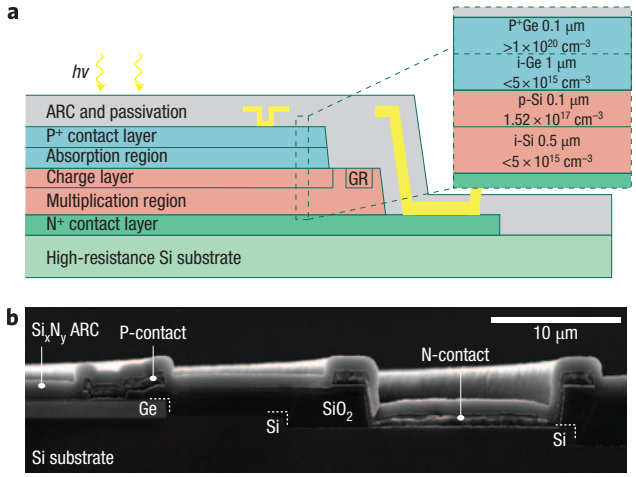

Figure 2 | **a**,**b**, Schematic (**a**) and SEM (**b**) cross-sections of a germanium/silicon APD. Doping concentrations and layer thicknesses were confirmed by secondary ion mass spectrometry (SIMS). The floating guard ring (GR in **a**) design was used to prevent premature breakdown along the device perimeter. ARC, anti-reflection coating.

Figure 1 presents a summary of experimentally measured gain–bandwidth products[15–28] with respect to multiplication layer thickness for different types of multiplication materials. One can see that when the multiplication layer thickness is similar, the gain–bandwidth product of silicon-based APDs (red data points) surpasses that of InP- and InAlAs-based APDs (black and green data points, respectively). InAlAs-based APDs with ultrathin multiplication layer thickness could achieve a high gain–bandwidth product but at the expense of complicated device design and very small process tolerances, making its viability for commercialization difficult. However, with silicon, an even higher gain–bandwidth product could be achieved based on a simple layer structure with relatively large process tolerances.

The germanium/silicon APDs presented in this work are based on the conventional separate absorption, charge and multiplication (SACM) APD structure in which light absorption and carrier multiplication occur inside germanium and silicon, respectively. A schematic and scanning electron microscope (SEM) cross-section of the mesa-type germanium/silicon APD are presented in Fig. 2. The room-temperature dark current and photocurrent of a typical 30-μm-diameter APD are shown in Fig. 3a. All tested devices exhibited a current–voltage characteristic typical of SACM APDs, with a clear rectifying behaviour. The punch-through voltage, corresponding to the voltage at which the depletion region penetrates into the germanium, is hard to extract from the current–voltage characteristics of our current devices because the punch through is close to the breakdown voltage. The punch through is therefore determined by the voltage at which the device capacitance reaches its minimum value of 77 fF. This agrees with the capacitance estimation when both germanium absorption and silicon multiplication regions are depleted. The punch-through voltage is ~ -22 V, with a responsivity of 5.88 A W^{-1} at 1,310 nm. The breakdown voltage V_{bd}, defined here at a dark current of 10 μA, occurs at -25 V. The breakdown voltage thermal coefficient (defined as $\delta = (\Delta V_{bd}/V_{bd})/\Delta T$, where ΔV_{bd} and ΔT are the increment of V_{bd} and temperature, respectively) is 0.05% °C^{-1} over a temperature range from 200 to 380 K. This value is typical for silicon-based APDs[29] and is about 70% and 30–50% that of the InAlAs- and InP-based APDs with similar layer structure[26,30–32], respectively. This decreased thermal sensitivity is another major advantage of silicon-based APDs as it will facilitate temperature stabilization of germanium/silicon APDs.

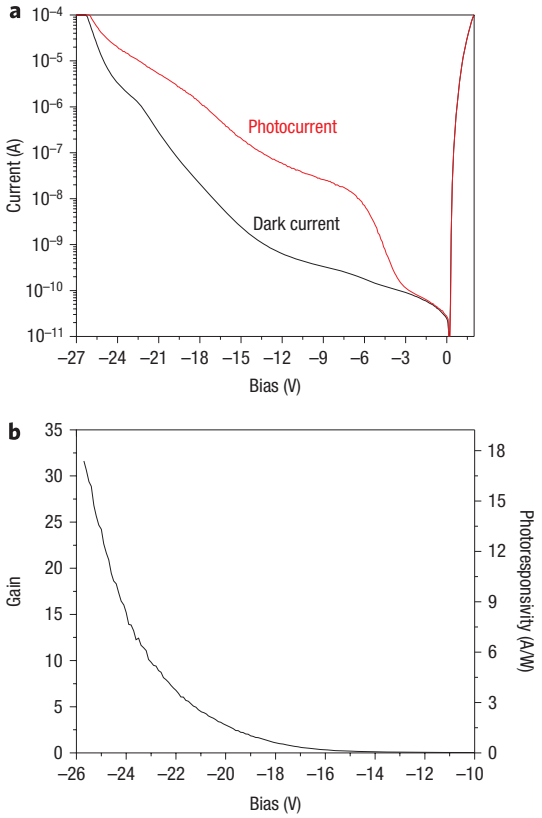

Figure 3 | Direct current characteristics of a germanium/silicon APD. **a**, The measured dark current (black curve) and total photocurrent (red curve) at room temperature of a typical 30-μm-diameter APD. **b**, The measured multiplication gain and photoresponsivity as a function of bias at a wavelength of 1,300 nm. The primary photoresponsivity used to obtain gain is 0.55 A W^{-1} measured from p–i–i–n devices fabricated on the same wafer as the APDs.

The dark current density is less than 19 μA cm^{-2} at biases up to -5 V and increases to 175 mA cm^{-2} when biased at 90% of breakdown voltage with a gain of 8. The measured dark current increases linearly with the device active area, suggesting that it is dominated by bulk leakage current. To understand more about the dark current generation mechanism, we also studied the dark current of the p–i–i–n device described in the Methods. The dark current density at -8 V is 18 mA cm^{-2}, which is comparable to germanium/silicon p–i–n results published by other groups[33,34]. Such a level of dark current density is an indication of good material quality and device fabrication. The dominating component of the dark current of the p–i–i–n device is the generation–recombination current that originates from dislocations at the germanium/silicon interface and inside the germanium film. For the APD case, we noticed that the primary dark current (dark current at unity gain that is multiplied by impact ionization at higher bias) is higher than the p–i–i–n dark current. We believe that the additional dark current is induced by the tunnelling current at the germanium/silicon interface, especially at high bias.

Figure 4a shows the excess noise factor versus gain, $F(M)$, extracted from a room-temperature noise measurement of a 30-μm-diameter germanium/silicon APD. Compared with McIntyre's model[14], plotted as solid lines in Fig. 4a, the estimated k_{eff} is $\sim$0.09.

The electrical 3-dB bandwidth of germanium/silicon APDs was measured using an Agilent 8703A Lightwave Network Analyser with its internal laser and modulator at 1,300 nm. Figure 4b plots

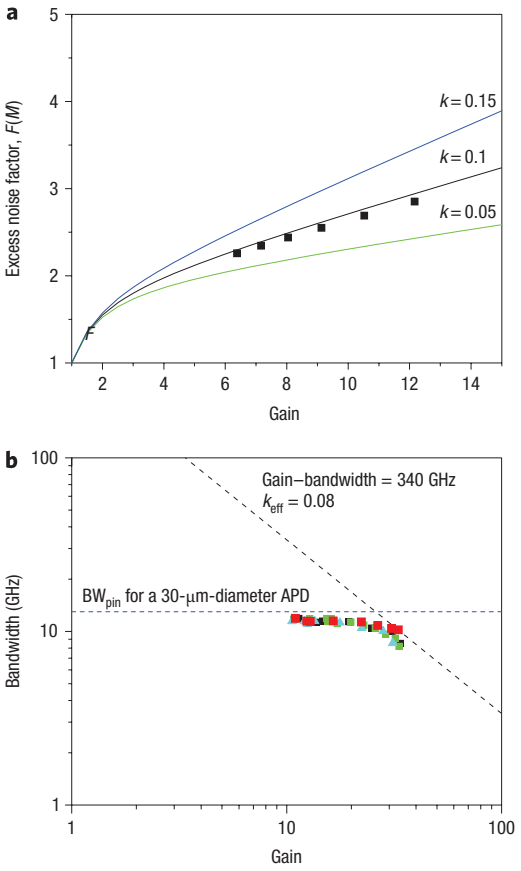

Figure 4 | Gain dependence of the excess noise and 3-dB bandwidth of the germanium/silicon APDs. a, Excess noise factor versus avalanche gain. The symbols represent the measured excess noise factor, and the lines are calculated values based on McIntyre's theory[14]. **b**, Measured 3-dB bandwidth versus gain of 30-μm-diameter germanium/silicon APDs at a wavelength of 1,300 nm. The coloured symbols are measured bandwidths from four devices. The blue line is the calculated bandwidth assuming carrier transit time and RC time constant are the limiting factors for the device bandwidth. The black line is a calculated result considering the avalanche build-up effect[13] with $k_{eff} = 0.08$. The corresponding gain–bandwidth product is 340 GHz, which fits the measured values. BW, bandwidth.

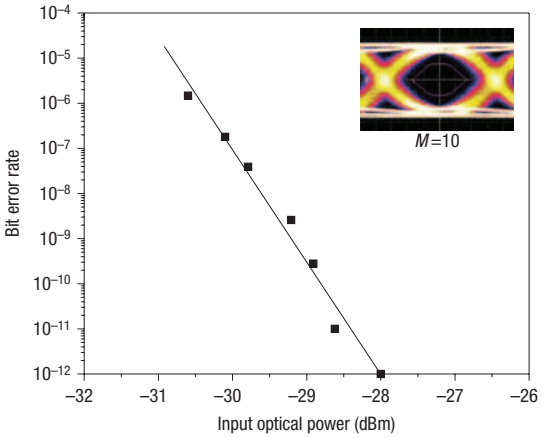

Figure 5 | Back-to-back receiver sensitivity and eye diagram measurements for a 30-μm-diameter germanium/silicon APD receiver measured at 10 Gb s^{-1}. The bit error rate is measured at the optimal bias voltage with 10 Gb s^{-1} non-return-to-zero PRBS optical pulses (word length $2^{31} - 1$) at 1,304 nm. The extracted receiver sensitivity is −28 dB m at a gain of 19, BER of 1×10^{-12} and ER of 12 dB. The inset is an eye diagram at a gain of 10 at −20 dB m input optical power.

the bandwidth as a function of gain from four 30-μm-diameter devices. For an APD operated at low gain, the bandwidth is limited by RC and transit time effects, which is similar to p–i–n photodiodes except that the depletion region includes both depleted germanium absorption and silicon multiplication layers. The maximum measured bandwidth is 11.5 GHz for gains up to 20, while theoretical calculations show that the bandwidth at low gain for a 30-μm-diameter device is 13 GHz, and is transit-time dominated. The minor difference between the measurement and the theoretical expectation most likely originates from parasitic effects, such as the insufficient contact layer doping concentrations and capacitance between the metal pads. However, the close-to-theoretical bandwidth at low bias voltage implies that the germanium/silicon interface has very limited effect on the device performance. As the gain is increased beyond 20, the bandwidth dropped owing to the avalanche build-up time effect[13]. All measured devices had a gain–bandwidth product over 300 GHz. The highest gain–bandwidth product obtained was 340 GHz. One should note that for InP APDs, the maximum usable gain at a data rate of 10 Gb s^{-1} is only 10–15 due to the low gain–bandwidth product, whereas this germanium/silicon APD has an optimal operational gain of over 30. Another point worth noting is that the k-value corresponding to a gain–bandwidth product of 340 GHz is ∼0.08 based on Emmon's model[13], which agrees very well with the value extracted from the excess noise measurement in Fig. 4a.

This high gain–bandwidth product and low k_{eff} are both significantly better than our previously reported results[35,36]. In those samples, the gain–bandwidth product and k_{eff} were 47 GHz and 0.4–0.5, and 153 GHz and 0.1–0.15, respectively. The higher performance of the APD devices presented here has been achieved mainly by redesigning the device doping profile and fabrication process to eliminate germanium impact ionization. In particular, the doping of the charge layer was increased to better confine the electric field inside the silicon, and the annealing temperature for the germanium was lowered substantially to reduce the interdiffusion of silicon and germanium. This prevents the germanium from diffusing into the gain region where it would increase the effective k. In addition, SEM cross-section analysis revealed a misalignment issue in the contact region, which resulted in an overetch of the germanium film for the previous work[36]. The unintended overetch led to a non-uniform carrier distribution, which resulted in earlier saturation of the gain–bandwidth product and, eventually, degraded device bandwidth performance. This has been corrected in the devices reported here. Finally, designs for a floating guard ring (GR) with various distances (1–3 μm) between the guard ring and the mesa edge were introduced to reduce the surface electric field strength at the silicon/insulator interface to prevent premature breakdown along the device perimeter. The floating GR is slightly different for our silicon/germanium APDs than in InP APDs. Because of the desire to keep the gain region relatively free of dislocations, the germanium film is on top of the silicon multiplication region. The placement of the GR is then buried at the silicon/germanium interface. This is different from what is typically found in InP APDs, which usually have the floating GR placed at the top surface. However, the fundamental physics of the floating GR is the same for both InP APDs[37] and germanium/silicon APDs. The dramatically improved gain–bandwidth product proves that the participation of the germanium in the carrier multiplication process is an extremely detrimental factor in germanium/silicon APD operation because germanium has a much higher k value. This gain–bandwidth product could be increased to over 400 GHz by further reducing the multiplication layer thickness.

In addition to measuring the gain–bandwidth product, we also measured the receiver sensitivity at 1,304 nm after packaging the germanium/silicon APD with a transimpedance amplifier (TIA). The germanium/silicon APD receiver was coupled to a standard, commercially available clock-data recovery circuit. Figure 5 shows a measured bit error rate (BER) curve of a receiver and the inset is an eye diagram at a gain of 10 and -20 dB m input optical power for a back-to-back experimental setup. At a data rate of 10 Gb s^{-1}, the receiver sensitivity was -28 dB m for 1×10^{-12} BER using a pseudo-random binary sequence (PRBS) word length of $2^{31} - 1$ and extinction ratio (ER) of 12 dB. This is the first germanium/silicon APD-based receiver to reach this level of performance. To the best of our knowledge, this result is comparable to the best commercial InP-based APD receivers and only $\sim$1 dB short of the best InAlAs-based APD receivers[30]. Assuming a higher primary responsivity of 0.85 A W^{-1} for the detector (this could easily be achieved by using a thicker germanium film or by moving to waveguide-based structures), we anticipate an improvement of approximately 1.8 dB in sensitivity.

To improve the sensitivity even further and to take advantage of the low noise and high gain–bandwidth product by using silicon as the multiplication region, there are at least two approaches that can be taken. The first is to reduce the dark current of the APDs. The primary dark current (calculated by total dark current divided by the gain at the optimal bias, assuming the unmultiplied dark current component is ineligible) of these devices is estimated to be less than 440 nA. Modelling shows that the receiver sensitivity improves when the primary dark current is reduced until a level of $\sim$100 nA is reached. Lowering the primary dark current below this threshold has no additional impact on the receiver sensitivity. An improvement in sensitivity of 1 dB is expected if our primary dark current is reduced to this level. We believe that the device dark current can be reduced by optimizing the device fabrication and design. In particular, better control of the germanium profile with respect to the electric field distribution in the device can reduce the tunnelling current. Moving to waveguide-based germanium/silicon APDs would also allow for detectors with an area approximately 10 to 100 times smaller than the current normal incidence devices, resulting in a corresponding reduction in the associated bulk-dominated dark current. A second approach for improving the sensitivity is to further reduce the value of k_{eff}. Simulation shows that a sensitivity improvement of over 1 dB is expected if k_{eff} decreases to 0.05. Studies have shown that k_{eff} can be reduced by optimizing the multiplication region thickness[38]. The challenge here would be to prevent germanium from contributing to the multiplication process and to find the optimal silicon multiplication thickness. Combining all of the improvements mentioned above, we believe that a sensitivity of approximately -32 dB m could be achieved. This is a 3-dB improvement over current state-of-the-art InAlAs APD receivers with the same measurement conditions (that is, a BER of 1×10^{-12}, 10 Gb s^{-1}, $2^{31} - 1$ data length).

In this paper, we have demonstrated a monolithically grown, CMOS-compatible germanium/silicon APD device with a gain–bandwidth product of 340 GHz and a k_{eff} of 0.09. The optical receivers built with the germanium/silicon APDs demonstrated a sensitivity of -28 dB m at 10 Gb s^{-1}. This is the highest gain–bandwidth product demonstrated for operation at a wavelength of 1,300 nm and the first reported monolithic germanium/silicon APD-based receiver that has such high sensitivity performance comparable to that of commercial III–V based APDs. These germanium/silicon APDs demonstrate that it is possible to build low-cost, CMOS-compatible, silicon-based devices that are superior in performance to APDs based on the traditional III–V materials. For instance, further device optimization can have 3 dB or more sensitivity improvement over commercial III–V APD receivers for 10 Gb s^{-1} operation. It is also possible to use this monolithic germanium/silicon-based technology to design APDs that operate at data rates of 40 Gb s^{-1} or higher where the performance of III–V APDs is severely limited. Outside the standard communication applications, one could now envisage new areas in biology and sensing where arrays of low-cost and highly sensitive receivers can fundamentally change how measurements are made.

Methods

Epitaxial growth and device fabrication. The device fabrication started with epitaxial growth on (100) silicon substrates, with a typical resistance of 20 Ω-cm, in a commercial chemical vapour deposition (CVD) chamber. All the silicon epitaxial layers were grown at 850 °C. The buried p-silicon charge region and floating GR were then simultaneously made by boron implantation with a dose of 1.5×10^{12} cm^{-2}. Later, a two-step germanium epitaxial deposition was used to minimize the misfit dislocation density due to the lattice mismatch. A relaxed, unintentionally doped germanium seed layer was grown at a lower temperature before the temperature was then increased to complete the growth of the layers. This procedure, followed by continuous or cyclic thermal treatment, has been demonstrated as an efficient way to reduce defect density inside germanium epilayers[39,40]. Etch pit studies on films overgrowing this annealed layer have shown a threading dislocation density of $\sim 5 \times 10^6$ cm^{-2}, as compared to a pre-annealing concentration larger than 1×10^8 cm^{-2}.

Circular mesas were dry-etched and then wet-etched through the germanium layer using a chemical mixture of H_2O_2:NH_4OH:H_2O and then dry-etched through the silicon epitaxial films to the silicon substrate. Immediately following the etching, the exposed mesa sidewalls were passivated with amorphous silicon and annealed at elevated temperature, in the range 700–900 °C. This step was done to further reduce the threading dislocation density inside the germanium. A silicon dioxide film was then deposited on top of the sample for planarization and to serve as an anti-reflection coating at 1,310 nm. Titanium/aluminium contact pads were formed on the top of the mesa and on the substrate. A coplanar waveguide (CPW) transmission line with characteristic impedance of 50 Ω was designed for high-speed measurement probing.

Multiplication gain. To determine the gain of the germanium/silicon APD, the primary responsivity was measured using a p–i–i–n device fabricated on the same wafer as the APDs. This device is essentially the APD structure but with no doping where the space charge region is normally located. The measured primary responsivity was 0.55 A W^{-1} at 1,310 nm, which agrees very well with the predicted value using 0.706 μm^{-1} as the absorption coefficient of germanium. The gain was obtained by normalizing the responsivity to the primary responsivity. Note that the gain at punch-through voltage is greater than unity. This means that there is some impact ionization occurring before punch through occurs. For practical applications, however, this is not an issue because the operational bias is always well above punch through.

Excess noise. The excess noise of the devices was measured as a function of multiplication gain, which was performed as follows. The device under test was biased using a stable voltage source. An optical continuous-wave laser source at 1,310 nm was used to illuminate the APD. The a.c. component of the device output (which is the noise of the photodiode in this case) was measured using a noise figure meter (HP 8970B). The total noise power density was obtained at 130 MHz, a frequency well above the $1/f$ noise regime. Careful system calibration was carried out to remove relative intensity noise and amplifier noise. The noise of the APD was then measured at various bias voltages. With known total current and gain at every bias point, the excess noise factor F was then extracted as a function of the gain M.

Received 9 June 2008; accepted 29 October 2008; published online 7 December 2008

References

1. Pavesi, L. & Guillot, G. *Optical Interconnect: The Silicon Approach* (Springer-Verlag, Berlin, 2006).
2. Reed, G. T. & Knights, A. P. *Silicon Photonic: An Introduction* (John Wiley & Sons, West Sussex, 2004).
3. Xu, Q., Manipatruni, S., Schmidt, B., Shakya, J. & Lipson, M. 12.5 Gbit s^{-1} carrier-injection-based silicon micro-ring silicon modulators. *Opt. Express* **15,** 430–436 (2007).
4. Liu, A. *et al.* High-speed optical modulation based on carrier depletion in a silicon waveguide. *Opt. Express* **15,** 660–668 (2007).
5. Huang, A. *et al.* A 10 Gb s^{-1} photonic modulator and WDM MUX/DEMUX integrated with electronics in 0.13 μm SOI CMOS. *Proc. IEEE International Solid-State Circuits Conference*, 922–929 (2006).
6. Morse, M., Dosunmu, O., Sarid, G. & Chetrit, Y. Performance of Ge-on-Si *p-i-n* photodetectors for standard receiver modules. *Proc. SiGe and Ge: Materials, Processing and Devices* **3,** 75–84 (2006).
7. Ahn, D. *et al.* High performance, waveguide integrated Ge photodetectors. *Opt. Express* **15,** 3916–3921 (2007).

8. Dehlinger, G. *et al.* High-speed germanium-on-SOI lateral PIN photodiodes. *IEEE Photon. Tech. Lett.* **16,** 2547–2549 (2004).
9. Boyraz, O. & Jalali, B. Demonstration of a silicon Raman laser. *Opt. Express* **12,** 5269–5273 (2004).
10. Rong, H. *et al.* A continuous-wave Raman silicon laser. *Nature* **433,** 292–294 (2005).
11. Sih, V. *et al.* Raman amplification of 40 Gb s^{-1} data in low-loss silicon waveguides. *Opt. Express* **15,** 357–362 (2007).
12. Fang, W. *et al.* Integrated AlGaInAs-silicon evanescent race track laser and photodetector. *Opt. Express* **15,** 2315–2322 (2007).
13. Emmons, R. B. Avalanche-photodiode frequency response. *J. Appl. Phys.* **38,** 3705–3714 (1967)
14. McIntyre, R. J. The distribution of gains in uniformly multiplying avalanche photodiodes: theory. *IEEE Trans. Electron. Dev.* **ED-19,** 703–713 (1972).
15. Campbell, J. C., Tsang, W. T. Qua, G. J. & Johnson, B. C. High-speed InP/InGaAsP/InGaAs avalanche photodiodes grown by chemical beam epitaxy. *IEEE J. Quant. Electron.* **24,** 496–500 (1988).
16. Yasuoka, N., Kuwatsuka, H. & Makiuchi, M. Large multiplication-bandwidth products in APDs with a thin InP multiplication layer. *Proc. 16th IEEE Annual Meeting of LEOS*, 999–1000 (2003).
17. Kinsey, G. S., Campbell, J. C. & Dentai, A. G. Waveguide avalanche photodiode operating at 1.55 μm with a gain–bandwidth product of 320 GHz. *IEEE Photon. Tech. Lett.* **13,** 842–844 (2001).
18. Lenox, C. *et al.* Resonant-cavity InGaAs–InAlAs avalanche photodiodes with gain–bandwidth product of 290 GHz. *IEEE Photon. Tech. Lett.* **11,** 1162–1164 (1999).
19. Hawkins, A. R., Wu, W., Abraham, P., Streubel, K. & Bowers, J. E. High gain-bandwidth-product silicon heterointerface photodetector. *Appl. Phys. Lett.* **70,** 303–305 (1996).
20. Kang, Y. *et al.* Fused InGaAs/Si avalanche phototodiodes with low noise performance. *IEEE Photon. Tech. Lett.* **14,** 1593–1595 (2002).
21. Clark, W. R. *et al.* Reliable, high gain–bandwidth product InGaAs/InP avalanche photodiodes for 10 Gb s^{-1} receivers. *Proc. Opt. Fiber Commun.* **1,** 96–98 (1999).
22. Franco, D. S. *et al.* High-performance InGaAs–InP APDs on GaAs. *IEEE Photon. Tech. Lett.* **17,** 873–874 (2005).
23. Li, N. *et al.* InGaAs/InAlAs avalanche photodiode with undepleted absorber. *Appl. Phys. Lett.* **82,** 2175–2177 (2003).
24. Yagyu, E. *et al.* Recent advances in AlInAs avalanche photodiodes. *Proc. Opt. Fiber Commun.* 145–147 (2007).
25. Nakata, T. *et al.* An ultra high speed waveguide avalanche photodiode for 40 Gb s^{-1} optical receiver. *Proc. 27th European Conference on Optical Communications* 564–565 (2001).
26. Rouvie, A. *et al.* High gain bandwidth product over 140 GHz planar junction AlInAs avalanche photodiodes. *IEEE Photon. Tech. Lett.* **20,** 455–457 (2008).
27. Makita, K., Nakata, T., Watanabe, I. & Taguchi, K. High-frequency response limitation of high performance InAlGaAs/InAlAs superlattice avalanche photodiodes. *Electron. Lett.* **35,** 2228–2229 (1999).
28. Hayashi, M. *et al.* Microlens-integrated large-area InAlGaAs–InAlAs superlattice APDs for eye-safety 1.5 μm wavelength optical measurement use. *IEEE Photon. Tech. Lett.* **10,** 576–578 (1998).
29. Su, Y. K., Chang, C. Y. & Wu, T. S. Temperature dependent characteristics of a PIN avalanche photodiode (APD) in Ge, Si and GeAs. *Opt. Quant. Electron.* **11,** 109–117 (1979).
30. Levine, B. F. *et al.* −29 dB m sensitivity, InAlAs APD-based receiver for 10 Gb s^{-1} long-haul (LR-2) applications. *Proc. Opt. Fiber Commun.* **6,** OFM5 (2005).
31. Ma, C. L. F., Dean, M. J., Tarof, L. E. & Yu, J. C. H. Temperature dependence of breakdown voltages in separate absorption, grading, charge and multiplication InP/InGaAs avalanche photodiodes. *IEEE Trans. Electron. Dev.* **42,** 810–818 (1995).
32. Hyun, K.-S. & Park, C.-Y. Breakdown characteristics in InP/InGaAs avalanche photodiode with *p-i-n* multiplication layer structure. *J. Appl. Phys.* **81,** 974–984 (1997).
33. Fama, S. *et al.* High performance germanium-on-silicon detectors for optical communications. *Appl. Phys. Lett.* **81,** 586–588 (2002).
34. Koester, S. J. *et al.* Temperature-dependent analysis of Ge-on-SOI photodetectors and receivers. *Proc. 3rd IEEE International Conference on Group IV Photonics*, 179–181 (2006).
35. Kang, Y. *et al.* Ge/Si avalanche photodiodes for 1.3 μm optical fiber links. *Proc. 4th International Conference on Group IV Photonics*, 294–296 (2007).
36. Kang, Y. *et al.* Epitaxially-grown Ge/Si avalanche photodiodes for 1.3 μm light detection. *Opt. Express* **16,** 9365–9371 (2008).
37. Liu, Y. *et al.* A planar InP/InGaAs avalanche photodiode with floating guard ring and double diffused junction. *J. Lightwave Technol.* **10,** 182–192 (1992).
38. Pauchard, A. R., Besse, P. A. & Popovic, R. S. Dead space effect on the wavelength dependence of gain and noise in avalanche photodiodes. *IEEE Trans. Electron. Dev.* **47,** 1685–1693 (2000).
39. Luan, H.-C. *et al.* High-quality Ge epilayers on Si with low threading-dislocation densities. *Appl. Phys. Lett.* **75,** 2909–2911 (1999).
40. Halbwax, M. *et al.* Kinetics of Ge growth at low temperature on Si (001) by ultrahigh vacuum chemical vapor deposition. *J. Appl. Phys.* **97,** 064907 (2005).

Acknowledgements

This work was sponsored by Defense Advanced Research Projects Agency (DARPA) under contract number HR0011-06-3-0009 and is supervised by J. Shah in the Microsystems Technology Office (MTO) office. The authors thank T. Liu, S. Yeh and C. Xie for assistance in device sensitivity measurements.

Additional information

Reprints and permission information is available online at http://npg.nature.com/reprintsandpermissions/. Correspondence and requests for materials should be addressed to Y.K.